

# FIRST SYNCHRONOUS MEASUREMENT OF SINGLE-BUNCHED ELECTRON AND POSITRON BEAMS WITH A WIDEBAND FEEDTHROUGH-BPM AT THE POSITRON CAPTURE SECTION OF THE SUPERKEKB INJECTOR LINAC

M. A. Rehman\*, T. Suwada, F. Miyahara  
High Energy Accelerator Research Organization (KEK),  
1-1 Oho, Tsukuba, Ibaraki 305-0801, Japan

## Abstract

The SuperKEKB is an asymmetric  $e^-/e^+$  collider with 40 times higher luminosity than the KEKB project, to explore the new physics beyond the standard model. For the SuperKEKB, the positrons are created by striking the accelerated electrons at a tungsten target. The secondary electrons are also produced during the positron creation process and accelerated in the capture section. Because of phase slipping in the capture section, the secondary electron bunch is only  $\sim 180$  ps away from the positron. Conventional stripline-type BPM cannot detect such closely spaced and opposite polarity signals due to slow frequency response and high cable losses. Therefore, a new wideband feedthrough-type beam position monitor was developed. It was successfully employed at the positron capture section of the SuperKEKB injector linac for the first synchronous measurement of the electron and positron beams. The cable losses effect also has been de-embedded to reveal correct signal properties. This paper describes the initial results of synchronous measurement of  $e^-/e^+$  transverse position.

## INTRODUCTION

The SuperKEKB (SKEKB) [1, 2] collider is currently under operation to study CP violation in B mesons and also to search for new physics beyond the Standard Model, with the target luminosity of  $8 \times 10^{35} \text{ cm}^{-2}\text{s}^{-1}$ , which is 40 times higher than its predecessor KEKB [3]. The SKEKB collider consists of electron ( $e^-$ ) and positron ( $e^+$ ) rings of energy 7 GeV (HER) and 4 GeV (LER) with the stored beam current of 2.6 A and 3.6 A, respectively.

The SKEKB injector linac provides  $e^-/e^+$  bunches of 5 nC and 4 nC to HER and LER respectively, at their designed energy. The low emittance  $e^-$  beam is produced by a RF-photocathode gun. The positron beam is produced by striking the  $e^-$  beam of energy 3.5 GeV and bunch charge of 10 nC at a tungsten target. The positrons are generated as secondary particles and have a large transverse emittance. To capture a large amount of positron, a pulsed solenoid called flux concentrator and a large aperture S-band (LAS) accelerating structure [4] are placed in the downstream direction of the positron target. The secondary electrons are also produced during the positron creation process and accelerated in the capture section. Because of phase slipping

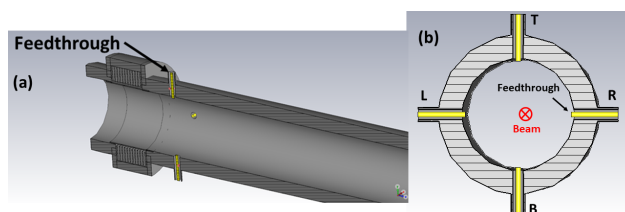


Figure 1: (a) The 3-D model of the new feedthrough-BPM. (b) Front view of the feedthrough-BPM, where "R", "L", "T" and "B" shows the right, left, top and bottom feedthroughs respectively.

in the capture section, the secondary electron bunch is only 180 ps away from the positron (depending on the phase of accelerating structure). Conventional beam monitors i.e. stripline-type BPM cannot detect such closely spaced and opposite polarity signals due to slow frequency response and high cable losses.

Therefore, new wideband feedthrough beam position monitor (BPM) was developed. And successfully employed at the positron capture section of the SuperKEKB injector linac for the first synchronous measurement of the electron and positron beams. This new monitor can detect  $e^-$  and  $e^+$  bunch properties i.e transverse position, bunch length, time interval, and bunch charges synchronously. It provides an opportunity to enhance positron transport through the capture section. The detailed analysis of bunch properties is reported in [6]. Here, we report the position response of feedthrough-BPM.

## FEEDTHROUGH BEAM POSITION MONITOR

The feedthrough-BPM consists of a vacuum pipe of length 431 mm and inner diameter of 38 mm, four SMA-type feedthroughs having inner conductor made of Kovar with  $\pi/2$  rotational symmetry are installed at the upstream direction of the vacuum pipe. The diameter of the feedthroughs is 1.8 mm and they extend 1 mm to the center of the beam pipe from the inner surface of the vacuum pipe. The vacuum pipe of BPM also has bellows installed at the downstream and upstream direction for flexible installation. The 3-D model of the new feedthrough-BPM and front view are shown in Fig. 1 (a) and (b), respectively.

\* rehman@post.kek.jp

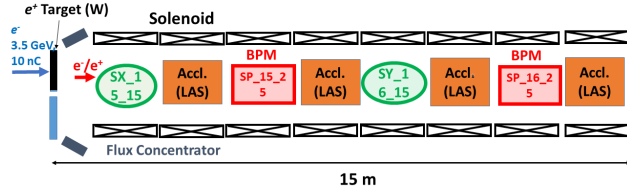


Figure 2: A schematic layout of the capture section depicting the position of new feedthrough-BPM and steering coils.

### Positron Capture Section

Two new feedthrough-BPMs namely SP\_15\_25 and SP\_16\_25 were installed in the positron capture section. The horizontal and vertical steering coils are also installed in the capture section to optimize the positron transmission through the capture section. Three horizontal and one vertical steering magnets have been installed in the  $e^+$  capture section. A schematic layout of the location of new feedthrough-BPMs and steering coils is shown in Fig. 2, a detailed description of the capture section can be seen at [6]. The horizontal and vertical steering coils labeled as SX\_15\_15 and SY\_16\_15 were used to observe the position response of feedthrough-BPMs. The entire capture section is enclosed in the DC solenoid coils for efficient transmission of large emittance positron beam.

### Coaxial Cable Losses

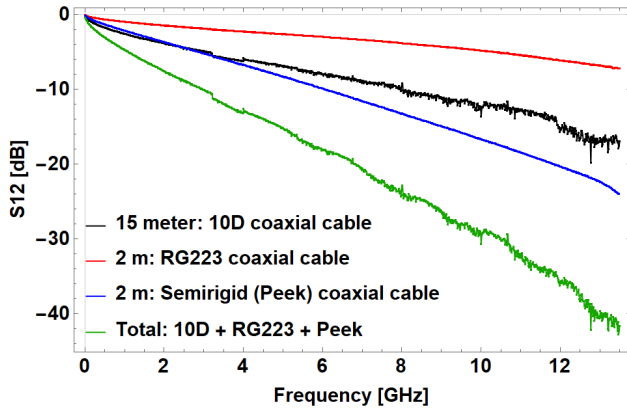


Figure 3: The coaxial cables losses at high-frequency measured by a vector network analyzer [8].

The SMA connector of the feedthrough is first connected to the 2 m long semirigid coaxial cable due to its protection against a high radiation environment. Later the semirigid cable was connected to the 15 m long 10D and 2 m RG223 coaxial cable [7]. The cable losses at high frequency were measured by a vector network analyzer [8]. A typical example of the high-frequency losses of coaxial cables is shown in Fig. 3.

The coaxial cables are then connected to a real-time keysight oscilloscope of bandwidth 33 GHz and a sampling rate of 128 GS/s [9]. The typical bipolar waveform at the nominal rf-phase from feedthrough-BPM is shown in Fig. 4.

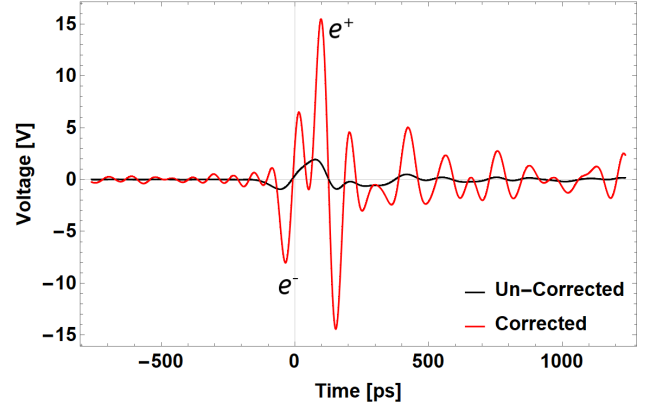


Figure 4: The synchronous signal of  $e^-/e^+$  at nominal accelerating phase from new feedthrough-BPM, the cutoff frequency was set to  $f_c = 10$  GHz.

The black curve in Fig. 4 shows the raw signal without any compensation of cable losses and due to high frequency losses in coaxial cable,  $e^-$  and  $e^+$  waveform are inseparable. Whereas, the red curve shows the case with high-frequency cable losses correction and  $e^-$  and  $e^+$  bunches can be distinguish from each other, the cutoff frequency for cable losses was set to 10 GHz.

When a charged particle travels through any obstacle (i.e. accelerating structure) it generates electromagnetic (EM) fields that left behind the particle. These left behind EM fields are called wakefield [10]. The wakefield can act on subsequent bunches transverse and longitudinal motion. In Fig. 4 a subsequent ringing waveform appear. This ringing waveform may be appeared due to the wakefields of both  $e^-$  and  $e^+$  bunches.

### SYNCHRONOUS MEASUREMENT OF $e^-/e^+$ BUNCHES TRANSVERSE POSITION

The area of the negative bulge of first (second) bipolar signal is considered for the  $e^-$  ( $e^+$ ) position measurement. The  $e^-/e^+$  beam position from feedthrough-BPM was analyzed by the difference-over-sum ratio ( $\Delta/\Sigma$ ):

$$x(y) = s_b \frac{A_r(A_r) - A_l(A_b)}{A_r(A_r) + A_l(A_b)}, \quad (1)$$

where  $A_r(A_r)$  and  $A_l(A_b)$  are calculated areas from the right (top) and the left (bottom) feedthroughs signals (see Fig. 1), respectively, and  $s_b$  is the BPM sensitivity given as:

$$s_b = \frac{R}{2}, \quad (2)$$

where  $R$  is the radius of the vacuum pipe. The transverse position change of  $e^-/e^+$  bunches at SP\_15\_25 and SP\_16\_25 are measured as a function of the field strength of horizontal and vertical steering magnet. The bunch charges were calculated by a summation of four pickup signals as given below:

$$Q = G \sum_i A_i, \quad (3)$$

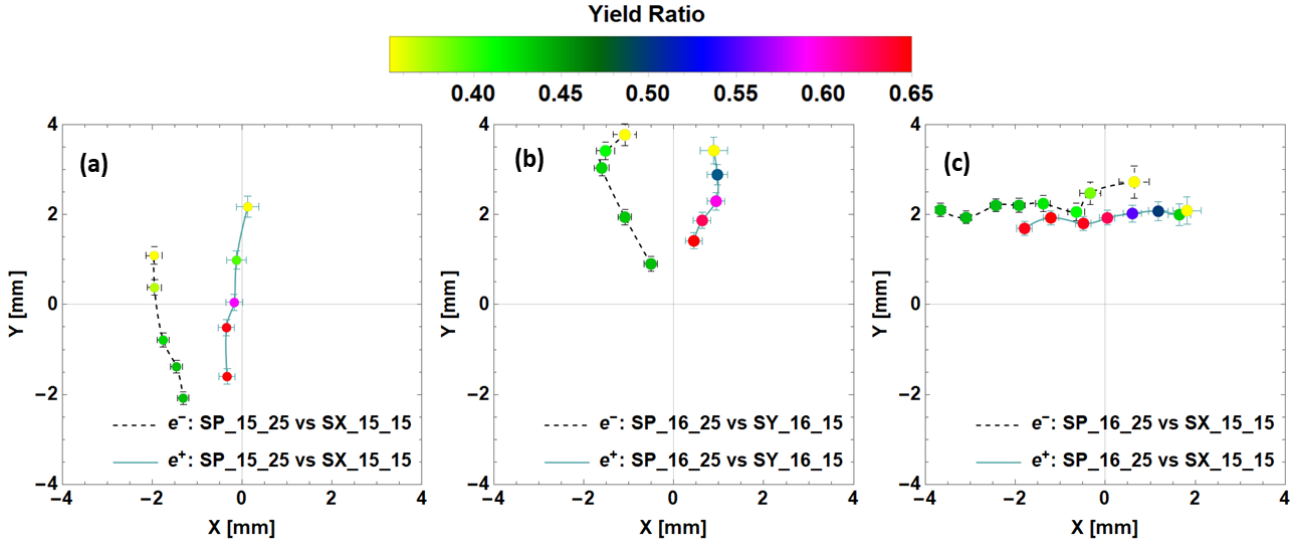


Figure 5: The synchronous transverse position of  $e^-/e^+$  measured by new feedthrough-BPM namely SP\_15\_25 and SP\_16\_25. The transverse position of  $e^-/e^+$  bunches were varied by the air-core horizontal and vertical steering magnets. The color band shows the positron yield variation due to the transverse position change of  $e^-/e^+$  bunches. (a) The transverse position change of  $e^-/e^+$  bunches at SP\_15\_25 with the horizontal steering magnet (SX\_15\_15). The transverse position change of  $e^-/e^+$  bunches at SP\_16\_25 with (b) the vertical (SY\_16\_15) and (c) horizontal (SX\_15\_15) steering magnets, respectively.

where  $Q$  is the beam charge and  $G$  is a conversion factor to calculate the beam charge. The detailed description is given in [6]. And the yield ratio is defined as the ratio of intensity of secondary produced bunch to the primary electron bunch.

Figure 5 shows the  $e^-/e^+$  bunches transverse position response as a function of the field strength of horizontal and vertical steering magnets and the color band in Fig. 5 corresponds to the  $e^-$  and  $e^+$  yield ratio. Figure 5 (a) shows transverse position change of  $e^-/e^+$  bunches at SP\_15\_25 with the horizontal steering magnet (SX\_15\_15). Figure 5 (b) and (c) presents the the transverse position change of  $e^-/e^+$  bunches at SP\_16\_25 with the vertical (SY\_16\_15) and horizontal (SX\_15\_15) steering magnets, respectively. When the strength of the horizontal steering magnet (SX\_15\_15) was changed the major position change in the vertical direction was observed at the SP\_15\_25 as shown in Fig. 5 (a). As explained in earlier section  $e^+$  capture section is enclosed in the solenoid to confine large transverse emittance  $e^+$  beam. This interesting beam motion arises due to the helical motion of charged particles under the solenoid field. When charged particles enter the solenoid field, they start rotating with the cyclotron period.

If the charged particle transverse position is observed at longitudinal position where the cyclotron period is not completed, then the position change will be observed in the opposite transverse position compared to the kick applied by the steering magnet. Whereas, at the full cyclotron period longitudinal position the transverse position change will be observed in the same direction as applied kick as observed in Fig. 5 (b) and (c). This interesting phenomenon was confirmed by the charged particle tracking (RK-4 method) under the solenoid field with the consideration of different kick

fields. The color band in Fig. 5 shows the  $e^-$  and  $e^+$  yield ratio as a function of the horizontal and vertical kick. This simultaneous information of bunch transverse positions and charges was used to optimize the  $e^+$  transmission through the positron capture section. The error bars on different transverse positions in Fig. 5 shows the systematic errors due to the frequency characteristics and wakefield effects. The frequency characteristics error is calculated by setting the different cutoff frequencies for high frequency cable losses. The error due to the wakefield in detail discussed in [6]. The total transverse position error is the root-mean-square sum of these two systematic errors, which is about 11%.

## SUMMARY

The first synchronous measurements of  $e^-$  and  $e^+$  bunches have been successfully performed with the wideband feedthrough-BPM system at the  $e^+$  capture section of the SuperKEKB factory. The synchronous transverse position and intensity of the  $e^-$  and  $e^+$  bunches were independently measured. The transverse motion of the  $e^-$  and  $e^+$  bunches was observed by the new feedthrough-BPM under the combined field of solenoid and steering magnets. The new wideband feedthrough-BPM proved as an excellent monitor to optimize  $e^+$  transmission through the  $e^+$  capture section.

## REFERENCES

- [1] K. Akai *et al.*, “SuperKEKB collider”, *Nucl. Instrum. Methods Phys. Res. A* 907, 2018, DOI: <https://doi.org/10.1016/j.nima.2018.08.017>.

- [2] Ohnishi, Y. *et al.*, “Accelerator design at SuperKEKB”, *Prog. Theor. Exp. Phys.* 03A011, 2013 DOI: <https://doi.org/10.1093/ptep/pts083>.
- [3] Abe, T. *et al.*, “Achievements of KEKB”, *Prog. Theor. Exp. Phys.* 03A001, 2013, DOI: <https://doi.org/10.1093/ptep/pts102>.
- [4] S. Matsumoto, T. Higo, K. Kakihara, T. Kamitani, and M. Tanaka, “Large-aperture Travelling-wave Accelerator Structure for Positron Capture of SuperKEKB Injector Linac”, in *Proc. 5th Int. Particle Accelerator Conf. (IPAC'14)*, Dresden, Germany, Jun. 2014, pp. 3872–3874, DOI: <https://doi.org/10.18429/JACoW-IPAC2014-THPRI047>.
- [5] N. Iida, H. Ikeda, T. Kamitani, M. Kikuchi, K. Oide, and D. M. Zhou, “Beam Dynamics in Positron Injector Systems for Next Generation B Factories”, in *Proc. 2nd Int. Particle Accelerator Conf. (IPAC'11)*, San Sebastian, Spain, Sep. 2011, paper THYA01, pp. 2857–2861.
- [6] Tsuyoshi Suwada, Muhammad Abdul Rehman, Fusashi Miyahara “First Simultaneous Detection of Electron and Positron Bunches at the Positron Capture Section of the SuperKEKB Factory”, *In review Sci. Rep.* <https://doi.org/10.21203/rs.3.rs-235736/v1>.
- [7] Catalog of high-frequency coaxial cables. <https://www.fujikura-dia.co.jp/>.
- [8] Keysight Technologies, Inc., N5230A PNA-L Network Analyzer. <https://www.keysight.com/en/>.
- [9] Keysight Technologies, Inc., UXR0334A Infiniium UXR-Series. <https://www.keysight.com/en/>.
- [10] Ferrario M., *et al.*, “Wakefields and Instabilities in Linear accelerators”, *Proc. CAS-CERN Accel. Sch. Adv. Accel. Physics, Trondheim, Norway, August 2013, edited by W. Herr (CERN-2014-009)*.